Nature and Dynamics of Lithium Ion Coordination in Oligo(ethylene glycol) Dimethacrylate-Solvent Systems: NMR, Raman, and Quantum Mechanical Study

J. Kříž,*,† S. Abbrent,‡ J. Dybal,† D. Kurková,† J. Lindgren,‡ J. Tegenfeldt,‡ and Å. Wendsjö§

Institute of Macromolecular Chemistry, Academy of Sciences of the Czech Republic, Heyrovsky Square 2, 162 06 Prague 6, Czech Republic, Institute of Chemistry, Uppsala University, P. O. Box 531, S-751 21 Uppsala, Sweden, and Danionics A/S, Hestehaven 21j, DK-5260 Odense S, Denmark

Received: April 29, 1999

Systems containing lithium bis(trifluoromethylsulfonyl)imide (TFSI), nona(ethylene glycol) dimetacrylate (EODM), and propylene carbonate (PC), or dimethyl sulfoxide (DMSO) in different concentrations were studied using ^{1}H, ^{6}Li, and ^{7}Li and ^{13}C 1D and 2D single quantum and double quantum filtered spectra, the corresponding longitudinal, transverse, rotating frame and $\mathbf{T}_1{}^3$ or $\mathbf{T}_2{}^3$ relaxations, Raman spectra, and quantum mechanical (MNDO up to ab initio SCF 6-31G and DFT) calculations. The mean, local, and exchange mobilities of the lithium ion as well as the apparent equilibrium constants of coordination to EODM (two stages) and the solvent were established. According to the study, the solvent in a gel electrolyte acts not only as a plasticizer but also as a competitive ligand loosening the coordination bond of the lithium ion to the poly(ethylene oxide) moiety. DMSO was found to be substantially more effective in this respect than PC.

Introduction

The possibility to use ion-doped polymers (polymer electrolytes) as electrolytes in electrochemical devices, and in particular, as a basis for high energy-density all-solid batteries has been the driving force behind numerous investigations of such systems.[1−6] In power source applications, the polymer electrolyte is required to have a high ionic conductance. The conductivity depends directly on the coordination and mobility of the ions present. Most work in the field of polymer electrolytes has dealt with monovalent ions and, in particular, with lithium ions. Interactions of the lithium cation with various ethylene oxide polymers or oligomers and their various derivatives designed as potential polymer electrolytes for industrial applications have been studied both experimentally and theoretically.[7−14] It is well-known that strong coordination of the lithium ion with poly(ethylene oxide) or its derivatives has desirable effects (good solubility of the lithium salt) as well as undesirable (suppressed mobility of the ion) and has to be finely tuned.

A way of increasing mobility is to add a plasticizing solvent such as propylene carbonate to the polymer, thus creating a polymer gel electrolyte. Following such a procedure the solvent was originally expected to coordinate the cations fully or to a great extent, decoupling them from the polymer network. This would enhance the ionic diffusion and thereby improve the conductivity of the system. To preserve the mechanical properties of the polymer, e.g., when it is used as an electrolyte membrane in thin film solid batteries, polymer gel electrolytes consisting of a relatively rigid three-dimensional network of a cross-linked polymer have been suggested. Cross-linked polymers based on radiation-polymerizable oligo(ethylene glycol) dimethacrylates have been one choice. We have earlier studied the lithium ion coordination in such systems and found that the lithium ions can be coordinated both to the plasticizer and to the oligo(ethylene glycol) chains.[15] We could, however, not decide anything from those experiments about the dynamics of the lithium ion coordination.

In the present study, we turn our attention to the system of nona(ethylene glycol) dimethacrylate (EODM) with lithium bis(trifluoromethylsulfonyl) imide (TFSI) and propylene carbonate (PC) or dimethyl sulfoxide (DMSO) as a solvent or plasticizer, designed as a precursor of a gel electrolyte. The advantage of studying the system before its polymerization lies in the possibility to utilize the powerful potential of high-resolution NMR. Some changes in the behavior after polymerization and cross-linking can be expected but the main features of the nature and dynamics of coordination should remain, at least qualitatively, the same. In fact, in a recent study the effect of polymerization on the coordination of metal ions in these systems has been investigated. UV−vis spectra of Nd^{3+} before and after polymerization were found to be virtually identical. This implied that the local coordination around the Nd^{3+} ion did not change on polymerization.[16] It was also found for the system dealt with in this paper, that on polymerization the coordination diminishes by around 20%, mostly due to steric hindrance introduced at the methacrylate cross-links. The local coordination of the cation remains the same as far as the FTIR spectra can reveal.[17]

The coordination of several metal ions, including lithium, has been studied by computational methods. It was found that a large number of different equilibrium coordination geometries with small energy differences occur.[12,18−20] To verify this for the present system, we have performed quantum mechanical calculations on lithium ion coordination in an EODM model system.

Experimental Section

Sample Preparation. The plasticizers propylene carbonate (PC, Merck, >99%) and dimethyl sulfoxide (DMSO, Mallinck-

* To whom correspondence should be addressed. E-mail: kriz@imc.cas.cz.
† Institute of Macromolecular Chemistry.
‡ Institute of Chemistry.
§ Danionics A/S.

10.1021/jp991410g CCC: $18.00
Published on Web 09/29/1999

rodt, Analytical reagent) and the oligomer nona(ethylene glycol) dimethacrylate (EODM, Aldrich) were dried with 3 Å silica molecular sieve. The salt lithium bis(trifluoromethanesulfonyl)-imide was dried in a vacuum oven at 100 °C for 48 h, and all chemicals were stored in a nitrogen filled drybox to avoid water contamination. The plasticizer content in the samples, expressed as the weight fraction of plasticizer with respect to total weight of polymer and plasticizer, was varied between 0 and 100 wt %. The samples so prepared were sealed into 5 mm precision tubes containing a concentric sealed capillary with D_2O as the locking substance.

NMR spectra and relaxation: ^{1}H, ^{13}C, ^{6}Li, and ^{7}Li spectra were measured at 300.13, 75.47, 44.17, and 116.64 MHz, respectively, with a Bruker Avance 300 DPX spectrometer. One-dimensional spectra were measured with 32 *k*points in a quadrature detection; for ^{13}C and ^{6}Li, exponential weighting was used before Fourier transform, the line broadening factor being 3.0 and 1.0 Hz, respectively. Homonuclear (COSY and NOESY) 2D spectra were measured with 1024 points and 256 increments, using quadrature detection in f2 and zero filling to 512 points in f1 dimension. Heteronuclear (HETCOR, HOESY) 2D spectra were measured with 1024 points and 128 increments with zero filling to 256 points in the f1 domain. Sine weighting functions were applied in both dimensions before Fourier transformation. Static ^{1}H→^{6}Li NOE experiments were done with a ^{1}H selective saturation (field intensity $\omega_1/2\pi = 8$ Hz). The T_1 measurements were done in the usual inversion−recovery regime modified by WALTZ decoupling during the whole sequence in the case of ^{13}C. For T_2 measurements, the Carr−Purcell−Meiboom−Gill sequence was used. $T_{1\rho}$ experiments were performed in the rotating frame using a pulsed spin-lock, the effective intensity of the applied locking field being calculated using the formula

$$\omega_1 = \pi\,[p_1/(p_1 + \Delta)]/(2P_1)$$

with p_1, Δ, and P_1 being the applied pulse length, the delay between pulses, and the length of the $\pi/2$ pulse at the given power level of the spin-lock field. For double-quantum-filtered (DQF) spectra, the sequence $\pi/2$-τ_1/2-π-τ_1/2-θ-τ_2/2-π-τ_2/2-θ-FID was used with a phase regime for DQF and the CYCLOPS phase cycling. θ was $\pi/2$ except for the pure T_1^2 tensor where θ was 54.72°. In the case of T_1^3 relaxation, τ_1 was incremented, the second π pulse was omitted, and τ_2 was 100 μs. In the case of $\mathbf{T}_2^3$ relaxation, τ_2 was incremented, the first π pulse was omitted, and τ_1 was 100 μs.

Raman spectra were measured in the same samples using a Bruker IPS-55 FTIR spectrometer with the Raman module FRA-106

Quantum mechanical calculations were performed in the MNDO, ab initio SCF 3-21G or 6-31G(d) and DFT (B3LYP functional) format using the Gaussian 94 program package.[21] The geometries of the molecules were fully optimized using the gradient optimization routine in the program, and all the stationary states were verified by inspecting their Hessian. The calculations were performed in C_1 symmetry.

Results and Discussion

1. ^{7}Li Single and Double−Quantum Spectra and Relaxation. In all systems containing LiTFSI (1.0−3.0 mol/L), oligo(ethylene oxide)-dimethacrylate (EODM), and propylene carbonate (PC) (10−90% w/w PC), ^{7}Li NMR gives a single signal with an almost perfect Lorentzian shape indicating that the extreme narrowing ($\omega_0\tau_c < 1$) condition is fulfilled. To ascertain this, the temperature dependence of T_1 for three different systems (100, 70, and 30% of PC in its mixture with EODM) was measured.

TABLE 1: Dynamic Parameters[a] of ^{7}Li Longitudinal Relaxation in LiCl−PC−EODM Systems

% PC	100	70	30
$\chi \times 10^{-8}$	6.77[0.42]	12.3[1.13]	15.2[1.35]
$\tau_0 \times 10^{15}$	1.61[0.23]	2.41[0.42]	5.48[0.82]
ϵ [kJ/mol]	26.6[2.41]	22.96[2.39]	27.3[2.62]
$\tau \times 10^{10}$ at 300 K	0.689[0.092]	2.4[0.18]	3.1[0.19]

[a] Error level in square brackets.

The typical T_1 values of ^{7}Li and ^{6}Li in the given system at 300 K are 0.4 and 8.3 s, respectively, whereas those of the relevant protons are around 0.5 s. Considering the former values in view of the ratios of the respective gyromagnetic ratios and quadrupole moments, $\gamma(^7\text{Li})/\gamma(^6\text{Li}) = 2.64$ and $Q(^7\text{Li})/Q(^6\text{Li}) = 56.25$, we can see that the relaxation mechanism for ^{7}Li is mostly quadrupolar although there is a small residual dipolar part present, too. In the following, we consider justified to assume, as an approximation, a fully quadrupolar relaxation.

The following expression[22] was fitted to the inverse−recovery data:

$$I_z(t) = I_z(0)[(1/5)\exp(-r_1 t) + (4/5)\exp(-r_2 t)] \quad (1)$$

where (*i* being subscript 1 or 2 in eq 1)

$$r_i = \chi \frac{\tau_c}{1 + (i\omega\tau_c)^2} \quad (2)$$

with $\chi = (1/10)[1+(1/3)a^2][e^2qQ/h]^2$, a being the asymmetry factor of the quadrupole coupling tensor and e^2qQ/h the quadrupole coupling constant. The correlation time was assumed to follow an Arrhenius temperature dependence, i.e.

$$\tau_c = \tau_{c0}\exp(\epsilon/kT) \quad (3)$$

ϵ being an activation energy of the motion decisive for the relaxation process. The values of χ, τ_{c0}, and ϵ fitted to experimental relaxation curves using eqs 1 and 2 for the systems are given in Table 1. Their interpretation is not simple due to the different viscosity of the measured systems. Nevertheless, one can say that the correlation times obtained are somewhat longer than expected for a simple rotational or translational diffusion, thus indicating some role of exchange even in longitudinal relaxation. The factor $\omega_0\tau_c$ at 116.64 MHz, however, is in the interval 0.05−0.23, i.e., the extreme narrowing condition is fulfilled and, consequently, relaxation is very nearly monoexponential, the value of T_1 has a physical meaning and its increasing value can be interpreted as a sign of a increasing mobility of the lithium ion. The quadrupolar coupling χ increases with larger concentration of EODM thus indicating anexpected lower symmetry of Li coordination.

With the values of τ_{c0} and τ_c obtained, it is permissible to approximate eq 1 by

$$I_z(t) = I_z(0)\exp\{-[(^1/_5)r_1 + (^4/_5)r_2]t\} = I_z(0)\exp(-R_1 t) \quad (4)$$

The temperature dependence of R_1 for the three systems studied is shown in Figure 1. All three curves go through a maximum shifted to a higher temperature with a higher EODM content. This is in agreement with the dynamic parameters in Table 1. At 300 K, we are in the decreasing region, i.e., near to the "extreme narrowing" condition, for all the systems consid-

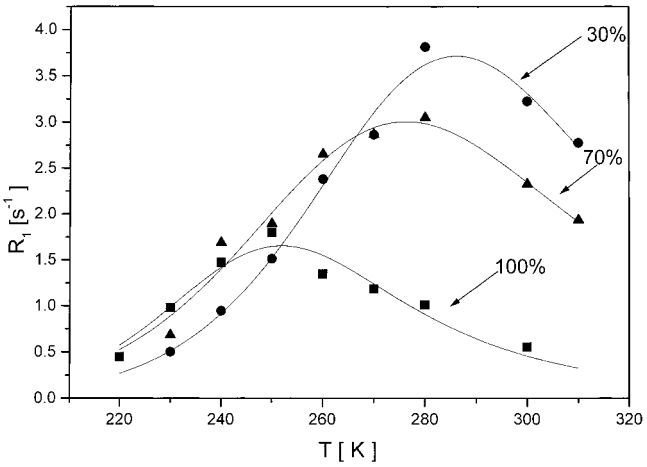

Figure 1. Temperature dependence of the ^{7}Li longitudinal relaxation rate in a 1 mol/L LiTFSI solution in EODM−PC mixtures at the indicated PC concentration (% w/w).

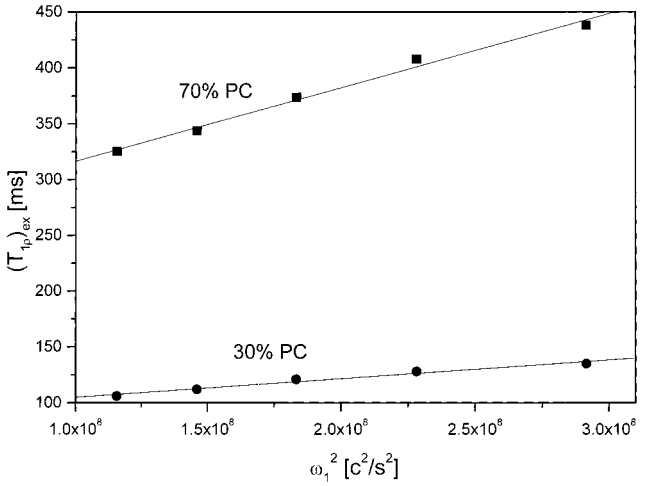

Figure 2. The linear dependence of ^{7}Li $T_{1\rho}$ on the square of the spin-lock field intensity in a 1 mol/L LiTFSI solution in EODM-PC mixtures at the indicated PC concentration (% w/w).

ered. This being so, the rotating-frame relaxation should obey the relation[23,24]

$$(T_{1\rho})_a^{-1} = (T_{1\rho})^{-1} - T_1^{-1} = \frac{\Delta\omega^2\tau_{ex}}{4(1+\omega_1^2\tau_{ex}^2)} \qquad (5)$$

where $(T_{1\rho})_a$ is the actually measured relaxation time, $\Delta\omega$ is the difference in chemical shift between the exchanging sites, $\omega_1 = \gamma B_1$ is the intensity of the spin-lock field expressed in rad/s, and τ_{ex} is the mean exchange correlation time,

$$\tau_{ex}^{-1} = \varphi_1\tau_1^{-1} + \varphi_2\tau_2^{-1} \qquad (6)$$

τ_i being the meantime of the Li residing on the φ_i-populated ith site. Relation 5 can be linearized[24]

$$(T_{1\rho})_a = \frac{4}{\Delta\omega^2\tau_{ex}} + \frac{4\tau_{ex}}{\Delta\omega^2}\omega_1^2 \qquad (7)$$

The plot of $(T_{1\rho})_a$ against ω_1^2 at 300 K for the systems containing 30 and 70% of PC is shown in Figure 2. As seen from eq 7, $\tau_{ex} = (B/A)^{0.5}$, B and A being respectively the slope and the abscissa of the linear dependence. The respective values of τ_{ex} for the two PC concentrations are 5.1×10^{-5} and 4.5×10^{-5} s, respectively, i.e., virtually the same considering the expected experimental error. This value near to 0.1 ms shows that there is lithium exchange even in the former case where almost all lithium is coordinated by OEDM, according to infrared spectra.[11] At the same time, however, it is at least 6 orders of magnitude longer than the usual correlation time of a diffusional jump, i.e., the lithium ion exchange crosses a marked energy barrier. Somewhat contrasting is the behavior of DMSO as a solvent. For DMSO/EODM = 3/7, $\tau_{ex} = 0.84 \times 10^{-5}$ s by the same technique, i.e., the exchange is about 10 times faster at the same temperature.

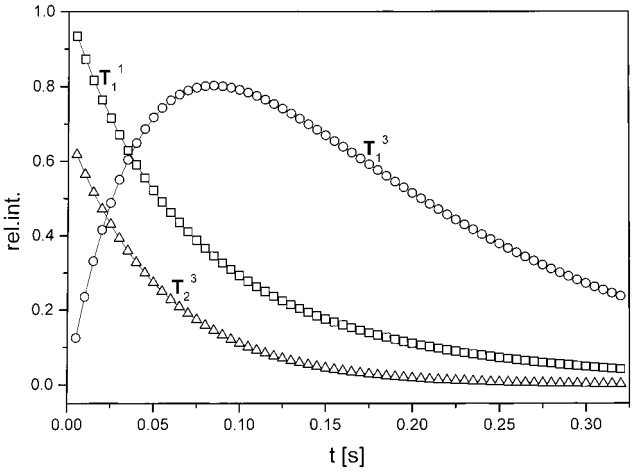

Figure 3. Time evolution of ^{7}Li $\mathbf{T}_1{}^1$ (rescaled 1/8), $\mathbf{T}_1{}^3$ and $\mathbf{T}_2{}^3$ in a 1 mol/L LiTFSI solution in a 1:1 w/w EODM−PC mixture.

Considering the ratio $\tau_{ex}/\tau_c \propto 10^6$ for the PC-EODM system, one should expect from the Lorentzian signal shape that either the mobility of the lithium ion coordinated to EODM is approximately equal to that solvated by PC or the former state is less mobile but its effect is hidden in the signal. We examined this possibility using double quantum filtered (DQF) ^{7}Li NMR spectra. It is known[25−28] that nuclei with spin $I > 1/2$ under certain conditions can form multipolar states described best in terms of irreducible spherical tensors[25,26] $\mathbf{T}_i{}^j$ differing in their rank j and order i. In the case of $I = 3/2$ (such as ^{7}Li), tensors $\mathbf{T}_1{}^2$ and $\mathbf{T}_1{}^3$ develop in time from the normal transverse magnetization $\mathbf{T}_1{}^1$, the former under static quadrupolar interaction (i.e., in a spatially anisotropic state), the latter, however, even under isotropic conditions providing the motion, is slowed-down beyond the extreme-narrowing condition. In other words, $\mathbf{T}_1{}^2$ is a measure of the *order* of the system, whereas $\mathbf{T}_1{}^3$ can be used to detect nuclei in a *relatively immobilized* state. Both $\mathbf{T}_1{}^2$ and $\mathbf{T}_1{}^3$ can be detected by transferring them by a $\pi/2$ pulse into the second-order states $\mathbf{T}_2{}^2$ and $\mathbf{T}_2{}^3$, filtering $\mathbf{T}_1{}^1$ off by the phase cycle and transferring the unobservable second-order states (or double-quantum coherences, DQC) to the observable $\mathbf{T}_1{}^1$ by another pulse and time delay. This procedure is referred to as double-quantum-filtered (DQF) spectra.

Despite the Lorentzian signal shape and the approximately fulfilled extreme narrowing condition, DQF spectra can be obtained with 160 or more scans for the systems containing less than 35% PC. The following analysis corresponds to 10% of PC in the system but analogous results can be obtained with concentrations somewhat higher (up to 35%). The longitudinal relaxation is apparently monoexponential, $T_1 = 0.231$ s at 300 K. The transverse (or single quantum) relaxation is again apparently monoexponential, $T_2 = 0.096$ s. Such a large discrepancy could be due partly to the exchange, partly to the magnetic field inhomogeneity caused by the inserted capillary with the locking substance. However, the existence of a DQF

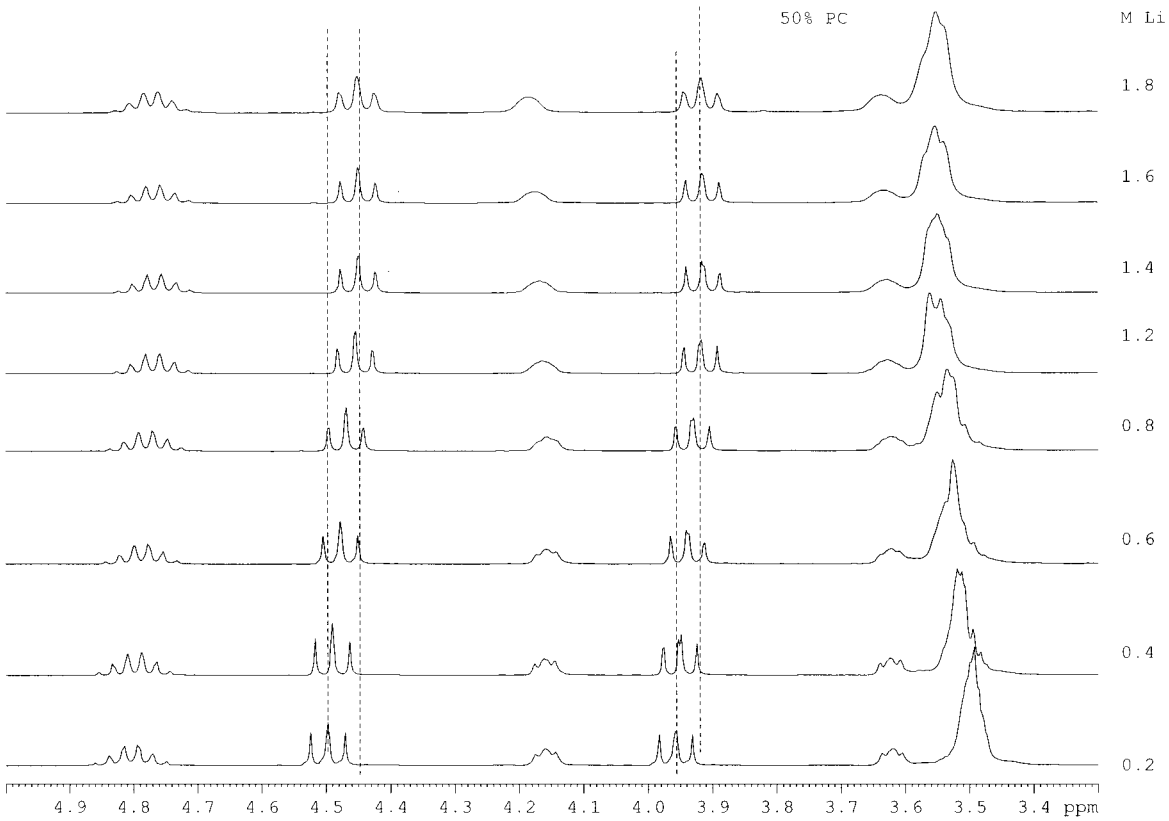

Figure 4. Relevant part of the ^{1}H NMR spectra of LiTFSI solutions in a 1:1 w/w EODM−PC mixture at the indicated LiTFSI concentrations.

signal indicates the relative immobilization of Li at its EODM coordination site to be a factor, as well.

In examining the DQC behavior, we first varied the length of the last two pulses in the sequence.[25] At 54.72°, the magic angle, the signal almost completely disappears, i.e., there is almost no static quadrupole coupling and the contribution of the second rank tensor[26] $\mathbf{T}_1^2$ is negligible. Thus we were able to follow the time evolution of the tensors $\mathbf{T}_1^3$ and $\mathbf{T}_2^3$ ($\mathbf{T}_i^j$ meaning the tensor of the jth rank and ith order) using the $\pi/2$ reading pulses[5] and adapting the pulse sequence accordingly.[27,28] Figure 3 shows the time evolution of $\mathbf{T}_1^1$ (downscaled 16 times), $\mathbf{T}_1^3$, and $\mathbf{T}_2^3$ (the evolution time of $\mathbf{T}_2^3$ in measuring $\mathbf{T}_1^3$ was 50 μs, that of $\mathbf{T}_1^3$ in measuring $\mathbf{T}_2^3$ was 15 ms). Neglecting dipolar contribution to relaxation,[27] the time development of $\mathbf{T}_1^3$ and $\mathbf{T}_2^3$ ($f_{31}^{(1)}$ and $f_{33}^{(2)}$, respectively) can be expressed[26−28]

$$f_{31}^{(1)} = (\sqrt{6}/5)[\exp(-R_s t) - \exp(-R_f t)] \quad (8)$$

$$f_{32}^{(2)} = \exp(-R_f t) \quad (9)$$

with $R_s = r_1 + r_2$ and $R_f = r_0 + r_1$ with r_j being defined in eq 2. The values of R_s and R_f obtained by fitting eq 8 to the corresponding curve were 7.2 and 18.02 s^{-1}, respectively, that of R_f obtained by fitting eq 9 was 18.10 s^{-1}, i.e., in a reasonable agreement with the previous result. It is easy to show that, for $q = R_f/R_s$,

$$\tau_c = \{(5q - 9) + [(5q - 9)^2 + 32(q - 1)]^{1/2}\}^{1/2}/(\sqrt{8}\omega_0) \quad (10)$$

Taking the value $q = 2.514$, we arrive at $\tau_c = 1.63 \times 10^{-9}$ s at 300 K, i.e., a value 1 order of magnitude higher than that obtained from the single or zero quantum relaxation. From this, one can conclude that at least at one of its coordination sites (EODM, without doubt), the lithium ion has a substantially lower mobility. As EODM is in excess in this system and its coordination ability is shown below to be substantially larger than that of PC, the low absolute intensity of the DQF signal indicates a marked interference of chemical exchange with this immobilization.

2. Structure of the Coordination Complexes: ^{1}H, ^{13}C, ^{6}Li, and ^{7}Li NMR, Raman Spectra, and Quantum Mechanical Calculations. In the systems containing the same amount of PC and EODM, both ^{1}H and in particular ^{13}C spectra change with increasing concentration of the lithium salt (Figures 4 and 5). An equally marked change can be observed under constant lithium concentration (1 mol/L) with increasing PC content (Figures 6 and 7). The most dramatic change can be observed in the signals of the CH_2O protons and carbons except those of the outer CH_2CH_2O units bonded to the methacryloyl groups. As shown in Figures 5 and 7, the ^{13}C signals of the remaining seven $-CH_2CH_2-O-$ units gradually shift and fan out into a variety of signals with changing intensities and positions reflecting their changing involvement in the lithium coordination. As the first shift of these signals already appears at low lithium concentrations (0.2−0.6 M, i.e., under large excess of both PC and EODM) without any trace of the signals from uncoordinated EODM, the observed patterns clearly reflect swift chemical exchange and equilibration of the individual signals.

For N exchanging sites, the shift of the equilibrated signal of the kth nucleus ν_k is a weighted mean of the shifts corresponding to the individual sites under no exchange, i.e.,

$$\nu_k = \sum_i^N p_{ki}\nu_{ki} \quad (11)$$

(where ν_{ki} is the original shift of the kth nucleus at the site i and p_i its relative population), provided that, for any i and j,

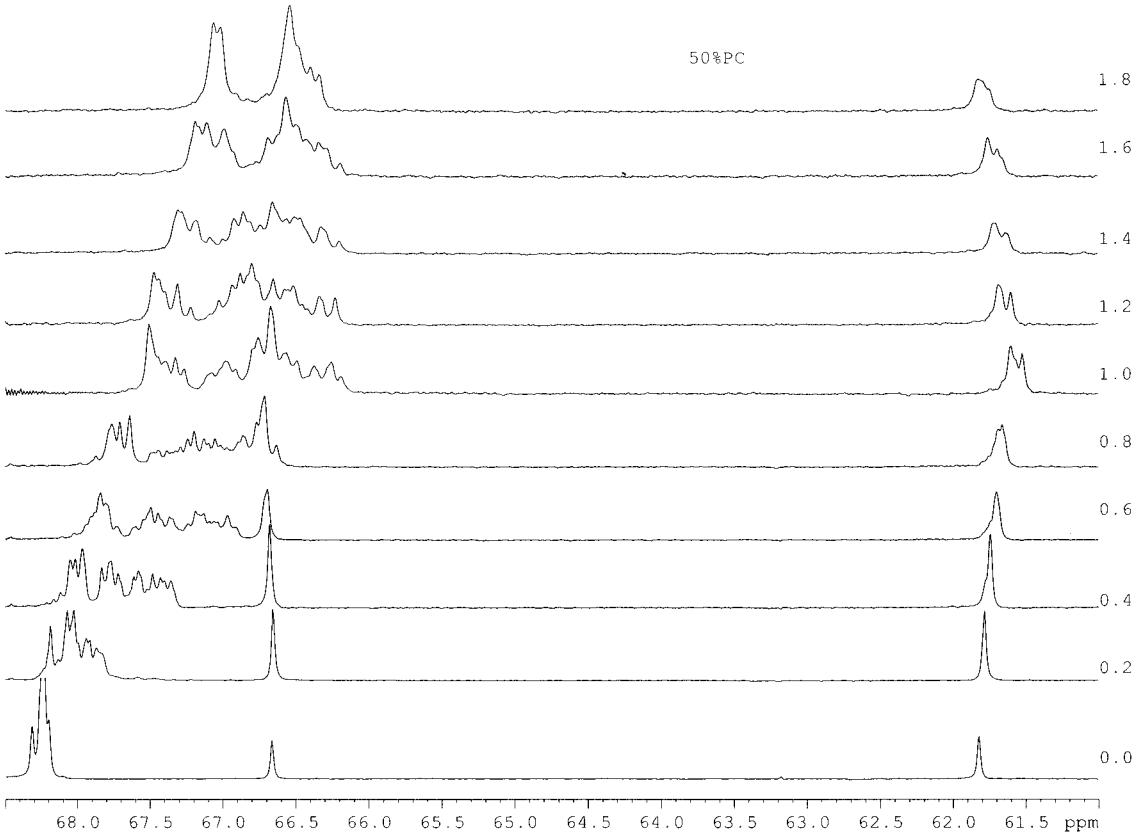

Figure 5. Relevant part of the ^{13}C NMR spectra of LiTFSI solutions in a 1:1 w/w EODM−PC mixture at the indicated LiTFSI concentrations.

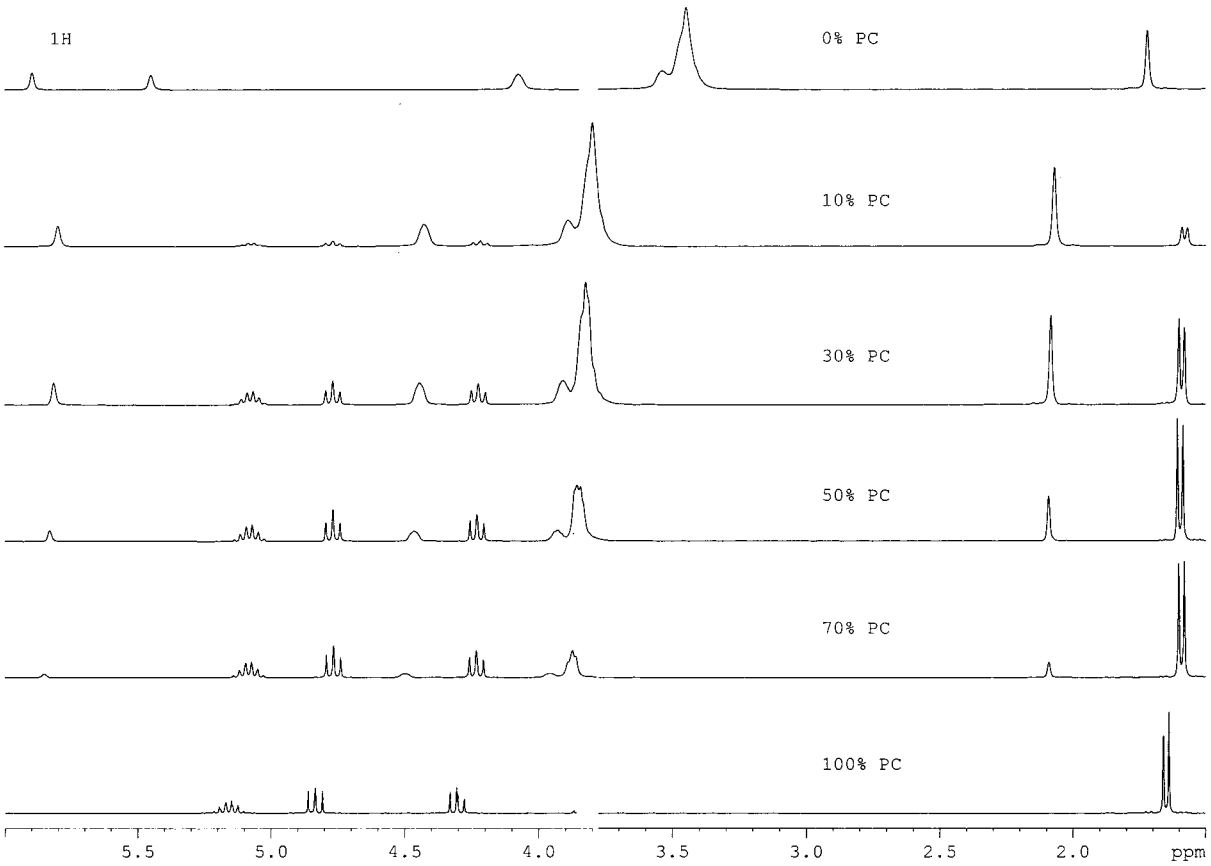

Figure 6. Relevant part of the ^{1}H NMR spectra of the 1 mol/L LiTFSI solutions in the indicated (% w/w) EODM−PC mixtures.

$2\pi|\nu_{ki} - \nu_{kj}|\tau_{ex} < 0.1$ (τ_{ex} being the exchange correlation time; the factor 0.1 at the right-hand side of this inequality is indicative of the order of magnitude at which the signals coalesce and narrow). Inspecting systems with an excess of both PC and EODM sufficient for the population of uncoordinated oligomer to be detectable, all nuclei in the inner $-CH_2CH_2-O-$ units

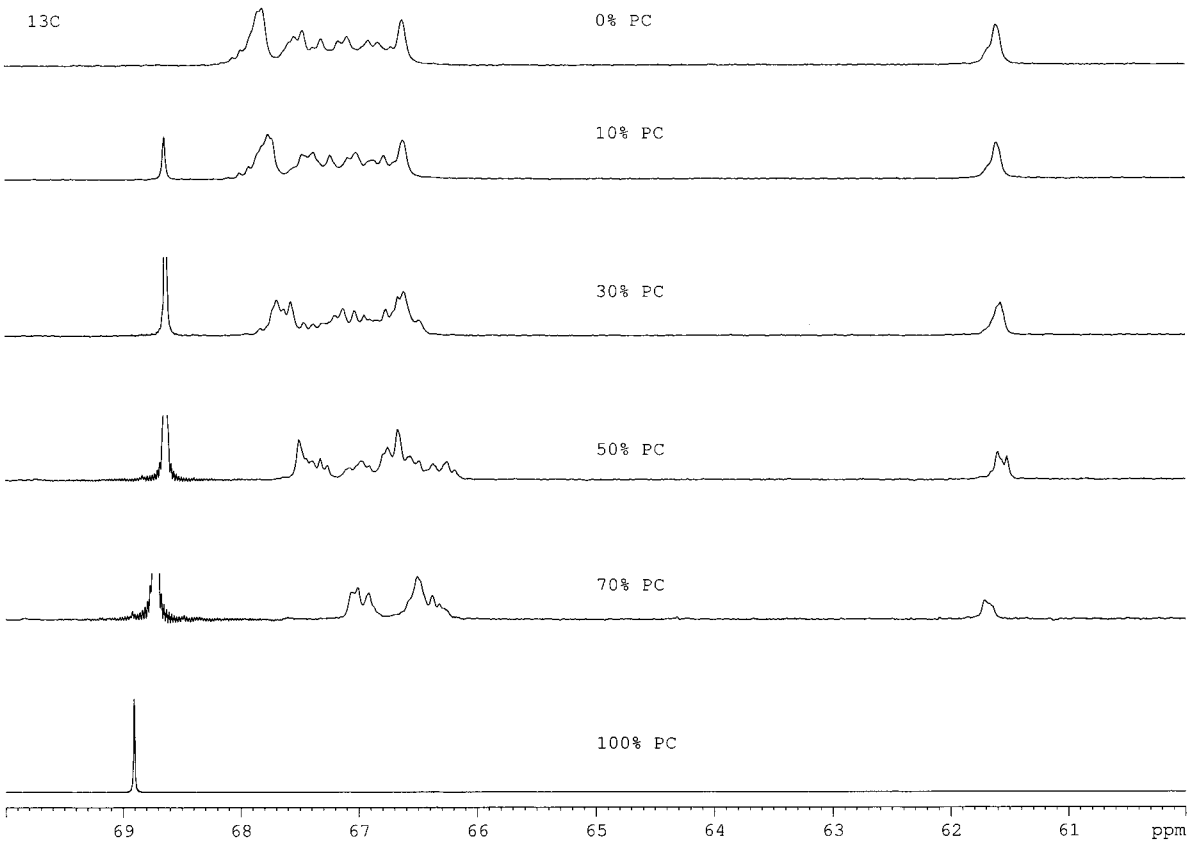

Figure 7. Relevant part of the ^{13}C NMR spectra of the 1 mol/L LiTFSI solutions in the indicated (% w/w) EODM−PC mixtures.

should have $|\nu_{ki} - \nu_{kj}| > 50$ Hz, i.e., $\tau_{ex} < 3 \times 10^{-4}$ s. Comparing this value to the previously determined correlation time of Li exchange of about 8×10^{-5} s, we can thus conclude that the changes in the $-CH_2CH_2-O-$ moieties are either synchronized with the jumps of the lithium atom or do not lag behind them to a very important degree. This conclusion is corroborated by the ^1H and ^{13}C relaxation measurements discussed below. The dependence of both positions and intensities of equilibrated signals on the relative populations of the respective exchanging sites (which change with increasing Li concentration due to progressive saturation of coordination ability of both PC and the innermost $-CH_2CH_2-O-$ moieties of EODM) makes the interpretation of the ^{13}C spectra extremely difficult. The following attempt is targeted at the system with 1.2 mol/L Li which clearly corresponds to the largest variety of ^{13}C signals. In this system, more than four PC molecules along with more than five inner oxygen atoms of EODM for each Li ion are still present, i.e., both types of ligands are able to coordinate lithium alone and compete according to their coordination abilities.

First of all, mutual exchange between the observed ^{13}C signals of the CH_2O groups was examined by both 2D ^{13}C NOESY and 1D selective-saturation experiments (since ^{13}C is of natural abundance, the probability of two ^{13}C nuclei in one molecule is about 10^{-4}, and direct as well indirect $^{13}C-^{13}C$ NOE effects were excluded). No exchange between observed signals was detected unequivocally, i.e., all the signals correspond to exchange equilibration of sites which we are not able to observe directly. Notwithstanding this, the change of ^1H and ^{13}C spectra under growing Li concentration indicates that the lower field proton and higher field carbon signals of the inner CH_2O groups correspond to atoms strongly affected by Li. We propose that the corresponding shift of ^1H and ^{13}C signals is not due merely to a different conformation of the incident bonds but also to a change in electron density in the bonding orbitals due to the vicinity of the lithium ion and the coordination bond of the nearest oxygen to it. Utilization of $^1H\rightarrow^7Li$ or $^1H\rightarrow^6Li$ NOE as an evidence of this conjecture is not easy due to the relaxation rate and mechanism of both lithium isotopes. As we argued earlier, the relaxation of ^7Li in our systems is mostly quadrupolar (i.e., relatively insensitive to NOE) whereas that of ^6Li is mostly dipolar (i.e., NOE sensitive). Unfortunately, the low natural abundance of both ^{13}C and ^6Li exclude the use of $^{13}C\rightarrow^6Li$ NOE leaving thus the use of NOE from the much less resolved proton resonances as the only possibility. Because the difference in T_1 values between ^1H and ^6Li were too large for a successful 2D $^1H\rightarrow^6Li$ HOESY spectrum, we used 1D ^1H-selective-saturation experiments (Table 2). The difficulty of this experiment is in the fact that half-widths (3.5−5.2 Hz) of the incident proton signals are comparable to their separation (7−15 Hz) so that an effective signal saturation always affects the nearest signal, too. In a viable compromise, we used a saturation field with ω_1 of about 7 Hz, which gives a measurable effect with minimum perturbation of the other signals. The results show clearly that the relatively low-field signals of the inner CH_2O groups (3.52 to 3.49 ppm) exert the strongest NOE to ^6Li, i.e., correspond to

TABLE 2: Net $^1H\rightarrow^6Li$ Equilibrium NOE Effects[a] Δ_{NOE} in a System EODM−PC with 1.0 mol/L LiTFSI and (a) 50 or (b) 70 % w/w of PC

	Δ_{NOE}	
δ (ppm)	*a*	*b*
3.645	0.02[0.005	0.06[0.005]
3.521	0.15[0.003]	0.12[0.003]
3.488	0.11[0.003]	0.10[0.003]
3.456	0.07[0.005]	0.08[0.005]

[a] $\Delta_{NOE} = I/I_0 - 1$, I_0 *is* the corresponding intensity in the unperturbed system; error level given in square brackets.

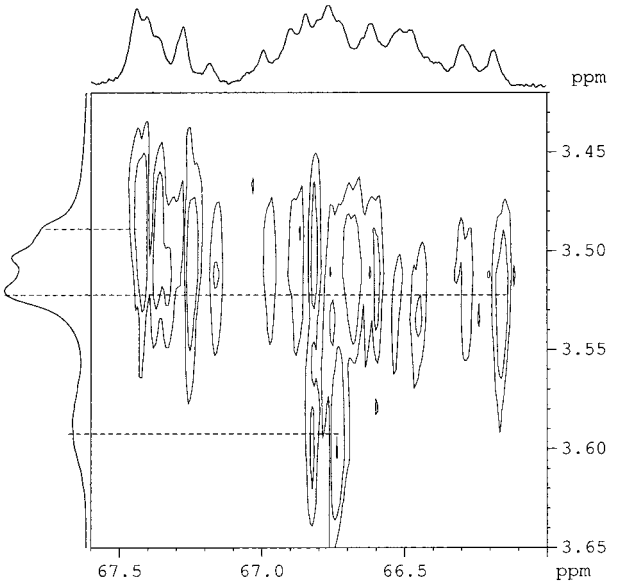

Figure 8. Relevant section of the $^{1}H-^{13}C$ HETCOR spectrum of the 1.2 mol/L LiTFSI solution in the 1:1 (w/w) EODM−PC mixture.

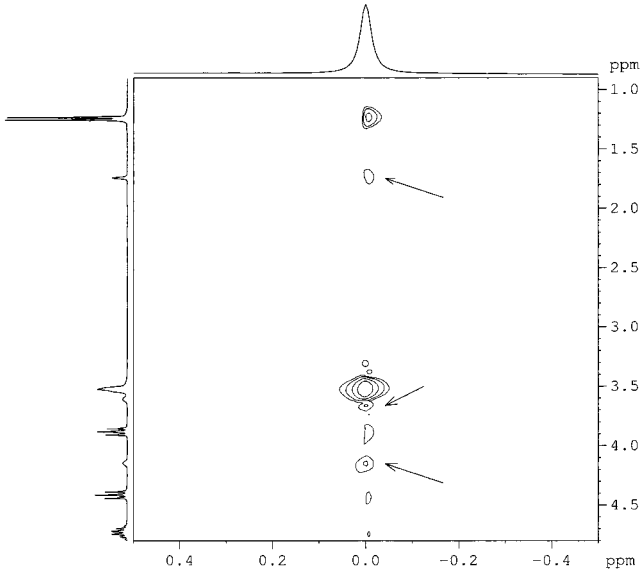

Figure 9. Relevant section of the $^{1}H-^{7}Li$ HOESY spectrum of the 1.0 mol/L LiTFSI solution in the 3:7 (w/w) EODM−PC mixture.

protons in nearest statistical vicinity to the lithium atom. Now, in a 2D $^{1}H-^{13}C$ HETCOR spectrum (Figure 8), one can see that the highest field ^{13}C signals correspond to the same situation, i.e., to the CH_2OCH_2 groups directly involved in the coordination.

From inspection of the proton spectra under increasing Li concentration from 0.8 to 1.8 M, we conclude that there are three different kinds of the inner CH_2O groups appearing in gradually changing relative populations. The shape of these signals indicates either an essential equivalence of the vicinal protons in the corresponding OCH_2CH_2O groups (i.e., symmetry of their vicinity) or their effective decoupling due to fast exchange. In the latter case, each of these signals would result from a dynamic equilibration. A perceptible shift of its position would be expected with its changing relative intensity unless each of the three main signals results from an independent equilibration. Apparently, the latter is indicated for the lithium concentrations from 1.2 to 1.8 M.

The complexity of the corresponding regions of the ^{13}C spectra is remarkable. As no slow exchange has been detected,

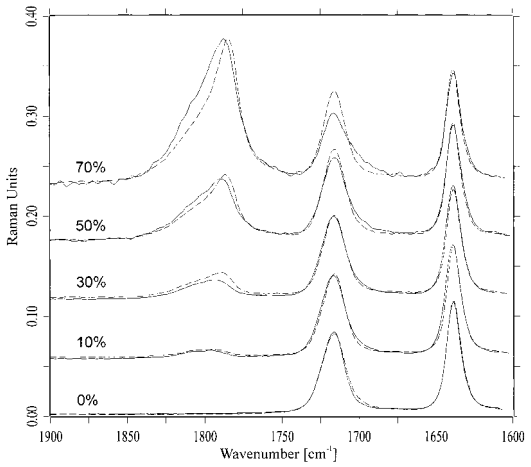

Figure 10. Relevant parts of the Raman spectra of the 1 mol/L LiTFSI solutions in the indicated (% w/w) EODM−PC mixtures compared with the (dashed) spectra of the same mixtures without LiTFSI.

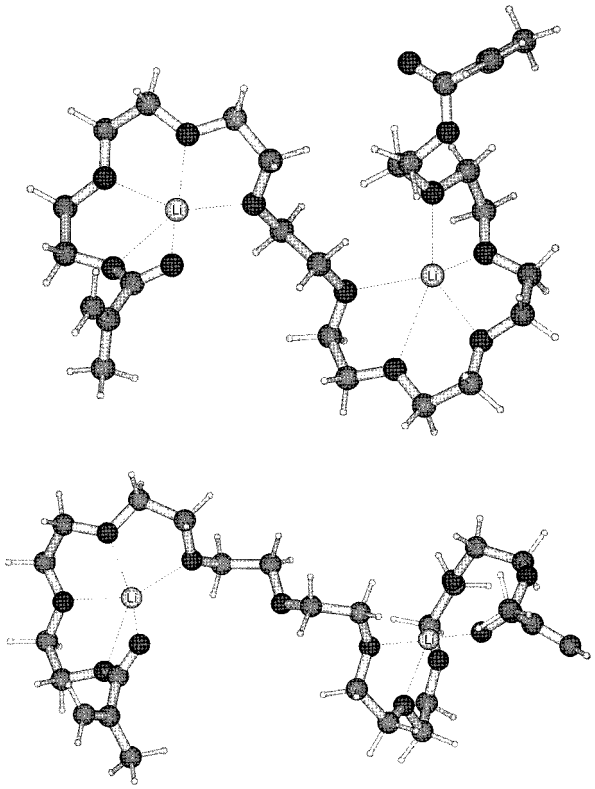

Figure 11. Two of the locally optimum geometries of the Li^{+}−EODM 1:1 and 2:1 coordinated structures according to MNDO.

every signal should be a result of fast equilibration between all sites present unless some exchange paths were excluded. Except the outer CH_2CH_2O groups directly attached to the methacryloyl groups, which have quite separate signals, we have 16 different CH_2O carbons in EODM, ignoring symmetry. The spectra for samples between 0.6 and 1.4 M Li indicate an even larger number of signals with varying intensity and line width. We are thus forced to conclude that several coordination forms coexist in the system, all of them exchanging rapidly with the uncoordinated molecules but some of them unable of even relatively slow mutual exchange. The gradual splitting of the ^{13}C signals of the ester CH_2O groups at higher lithium concentrations points to the same conclusion.

An interesting twist is offered by the system containing 1.0 M Li at the PC/EODM weight ratio less than 0.5. As already indicated in Table 2, the ester $-OCH_2-C\mathbf{H}_2O$ protons have a

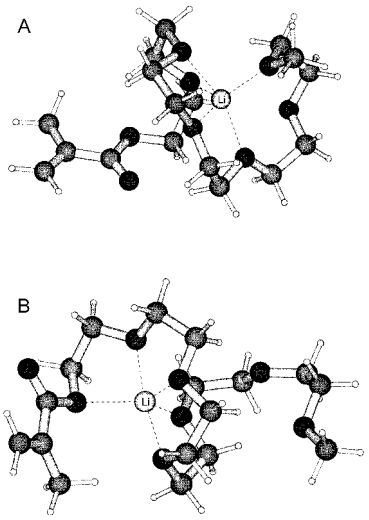

Figure 12. Two locally optimal geometries of the Li^+ coordination with the methyl ether of hexa(ethylene glycol) methacrylate.

marked NOE on ^{6}Li, in contrast to lower PC concentrations. In a ^{1}H→^{7}Li HOESY spectrum shown in Figure 9, NOE cross-peaks appear not only for inner CH_2O but also for both types of OCH_2-CH_2O ester protons and even for the methacryloyl methyl signal (cross-peaks with arrows). This is in contrast to HOESY spectra of an equal number of scans measured with 50% and lower concentrations of PC. A detectable though slight shift can be observed for both OCH_2-CH_2O ester carbons as well as for the ester carbonyl signal. In Raman spectra (Figure 10), a clear broadening or shoulder on the ester carbonyl band (1717 cm^{-1}) associated with the presence of LiTFSI can be observed at PC contents higher than 50%. From difference spectra, 23 and 6 % mol of the ester groups are in the coordinated state at 70 and 50 % PC, respectively, i.e., this coordination increases with increasing relative PC concentration.

All these observations indicate an increasing involvement of the methacrylate group in the lithium coordination at PC concentration increasing over 50%. In principle, such a phenomenon could be due to three different causes: (i) PC as a medium promotes a coordination form involving one of the ester groups; (ii) PC at its higher concentration shares coordinated lithium with EODM and the most stable form of the mixed complex involves ester coordination, (iii) the EODM molecule can coordinate two lithium ions (which happens at low concentrations of EODM), one of them being bound partly to the ester group.

Of these possibilities, the quite strong cross-peaks between the PC protons and Li in the HOESY spectrum (Figure 9) along with those of EODM protons seem to support case (ii). However, any attempt to detect ^{1}H−^{1}H NOE between PC and EODM by NOESY (including a weekend experiment) failed. This diminishes the probability of (ii) although it cannot be regarded as a real refutation considering the steep r^{-6} dependence of NOE and the geometry of the hypothetical complex.

Regarding (iii), one has to consider the fact that the number of EODM molecules per lithium ion is less than one above 43.9% and less than one-half above 75.0% of PC. In other words, in the case of a large coordination preference of EODM against PC, some of the EODM molecules have to coordinate two lithium ions above 43.9% of PC. We examined this possibility by quantum calculations. EODM is too large for any precise method, but according to our MNDO calculations, two lithium ions are easily coordinated by one EODM molecule. The system offers quite a variety of local energy minima so that, considering also the possible artifacts of the MNDO method, the exact energy balance is scarcely attainable. As

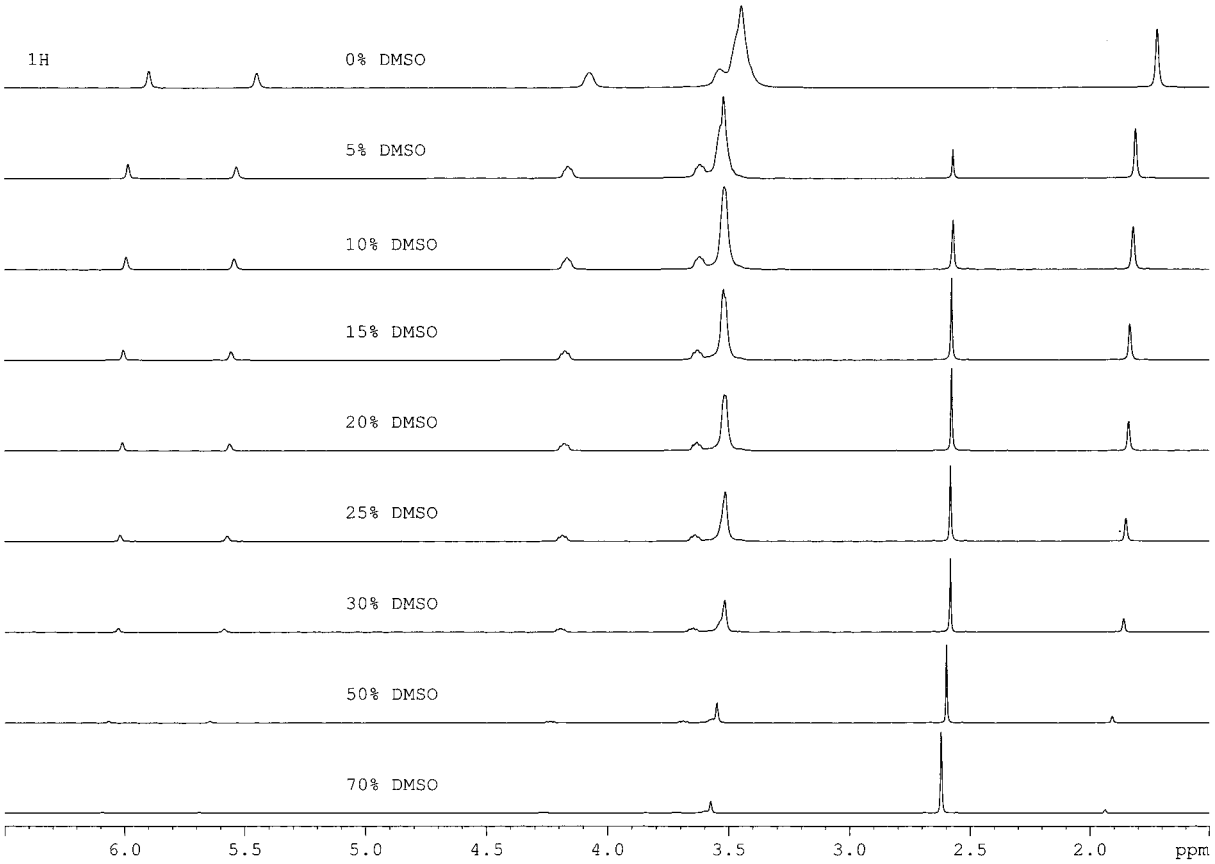

Figure 13. Relevant parts of the ^{1}H NMR spectra of the 1 mol/L LiTFSI solutions in the indicated (% w/w) EODM−DMSO mixtures.

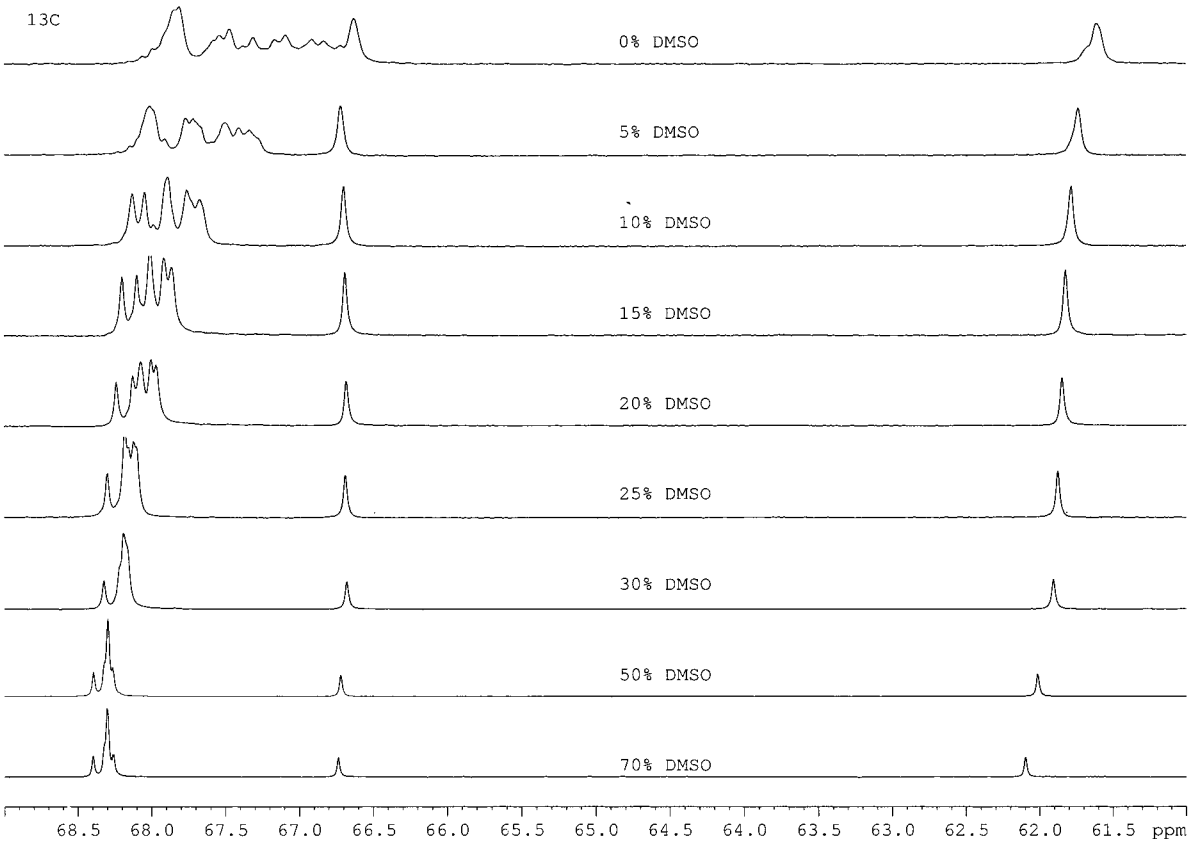

Figure 14. Relevant parts of the ^{13}C NMR spectra of the 1 mol/L LiTFSI solutions in the indicated (% w/w) EODM−DMSO mixtures.

shown in Figure 11, however, the form including exclusively inner oxygen atoms as well as that including the ester group is predicted to be relatively stable. To gain a somewhat more exact idea of the stability of different coordination sites at the EODM molecule, we performed state-of-the-art calculations at the ab initio SCF 6-31G and the DFT level. As the EODM molecule was too large for such a treatment, we used the methyl ether of hexa(ethylene glycol) methacrylate as a nearest model. Geometry optimizations were performed at the HF level using the 3-21G basis set. The energies of the optimized systems were finally evaluated at the DFT level of theory (B3LYP/6-31G*//HF/3-21G). The optimal geometry of the two alternative coordination sites are shown in Figure 12. The complex with purely oxyethylene coordination sites (A) is energetically more favorable by 7.0 kJ/mol in comparison with ester-involving (B) coordination sites. We thus see that the two sites are quite comparable in stability. The reason we do not observe site B at higher EODM concentrations must be purely statistical: there are four sites A and at least 6 analogous, only slightly less stable coordination sites in a EODM molecule for one lithium ion.

The system behaves quite differently if it contains DMSO instead of PC. As shown in the ^{1}H and in particular ^{13}C NMR spectra in Figures 13 and 14, respectively, there are mere traces of EODM coordination at the DMSO/EODM ratio $\alpha = 3/7$. At $\alpha = 1$, EODM appears to be completely stripped of lithium ions. The spectra clearly reflect more than a simple competition between EODM and DMSO. As seen in Figure 14, a quite dramatic change already appears at $\alpha = 5/95$, i.e., at 0.58 mol/L of DMSO. As at least four DMSO molecules are needed to coordinate the lithium ion completely, less than 15% of the full lithium content can be permanently coordinated to DMSO, which as such should not affect the spectrum in such a substantial way. Evidently, there must be a very fast exchange between the EODM and DMSO coordination sites. The change of the spectra in the interval of α from 1/9 to 25/75 where the pattern is analogous but the shift of the signals is changing is in accord with this interpretation. The same conclusion follows from the above ^{7}Li rotating-frame relaxation measurements showing the exchange between EODM and DMSO to be about 10 times faster than that between EODM and PC.

3. Analyzing the Coordination Equilibria Using ^{13}C NMR Relaxation. Let us assume the existence of only two different states of the solvent, namely free and coordinated. Under fast exchange (warranted by the gradual change in the relative shift of the solvent signals in the mixtures containing their increased fraction), we can use the following relation for the experimental relaxation time T_1:

$$T_1^{-1} = \varphi_s T_{1s}^{-1} + (1 - \varphi_s) T_{1cs}^{-1} \tag{12}$$

where φ_s is the molar fraction of the uncoordinated state in the total solvent, T_{1s} and T_{1cs} are the relaxation times in a pure solvent and in the coordinated state, respectively. From this, φ_s can be extracted:

$$\varphi_s = \frac{(T_{1s} - T_{1cs})T_1}{(T_1 - T_{1cs})T_{1s}} \tag{13}$$

Assuming now that n molecules of the solvent coordinate one Li with an equilibrium constant K_s whereas one ligand molecule can coordinate one or two ions with the constants K_1 and K_2, we can write:

$$K_s = \frac{(1 - \varphi_s)C_s}{n\varphi_s^{\,n} C_s^{\,n} C_{fLi}}; \quad K_1 = \frac{C_I}{C_{If} C_{fLi}}; \quad K_2 = \frac{C_{II}}{C_I C_{fLi}} \tag{14}$$

where C_s, C_I, C_{II}, C_{Lf}, and C_{fLi} are the molar concentration of

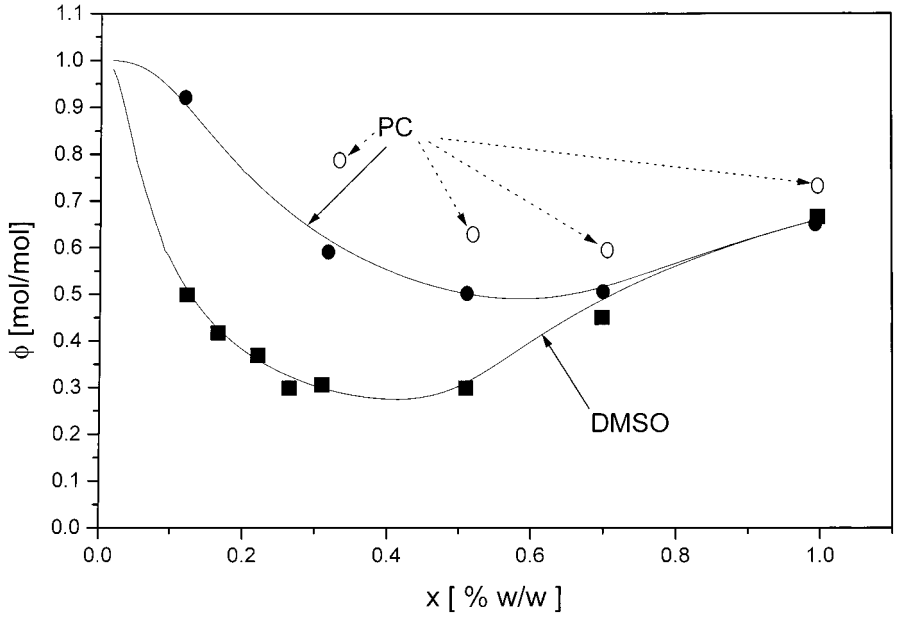

Figure 15. Fitted experimental values of the free solvent molar fractions obtained from ^{13}C T_1 relaxation data of 1 mol/L solutions of LiTFSI in PC (●) and DMSO (■). The ○ points indicate the results obtained from Raman spectra.

the solvent, the ligand complex with one and two coordinated ions, the free ligand, and the uncoordinated Li, respectively. After elementary manipulations, we arrive at the implicit equation for φ_s:

$$\frac{(1-\varphi_s)C_s}{n} = C_{Li} - \xi - \frac{K_I C_I \xi(1+2K_2\xi)}{1+(1+K_2\xi)\xi} \tag{15}$$

with

$$\xi = \frac{(1-\varphi_s)}{n\varphi_s{}^n C_s{}^{n-1} K_s} \tag{15a}$$

where C_L and C_{Li} are the total molar concentrations of the ligand and the lithium salt, respectively. Equation 15 has to be solved numerically but can serve for optimizing the parameters n, K_s, K_1, and K_2.

In the case the solvent forms a mixed complex with lithium and the ligand in the sense of an additional equilibrium

$$K_3 = \frac{C_{III}}{C_{If} C_{fLi} C_s} \tag{16}$$

the analysis is even more cumbersome and leads to the implicit equation

$$\frac{nC_{Li}\sigma - (1+\sigma)(1-\varphi)C_s}{C_s(K_I+\beta C_s)(1-\varphi) - \beta C_{Li}} + \frac{\zeta - \{\zeta^2 - 4\beta C_s[n\sigma(C_{Li}-C_I) + (1+\sigma)(1-\varphi)C_s]\}^{1/2}}{2\beta C_s} = 0 \tag{17}$$

where $\zeta = (C_{Li} - C_L)C_s\eta + n\sigma$, $\sigma = K_s\varphi^n C_s{}^n$, $\beta = K_1K_3\,\varphi$, the other symbols being the same as above.

The difficulty arising with the use of eq 13 is the marked dependence of the relaxation time T_1 on the viscosity of the system increasing with the decreasing content of the solvent. To overcome this problem, we used the following approximation. The correlation time of the rotational diffusion can be approximated by the Debye relation

$$\tau_r = 4\pi R_d{}^3\eta/3kT \tag{18}$$

where R_d is the rotational diffusion profile of the molecule, η is the viscosity, k is the Boltzmann constant, and T is temperature. At extreme narrowing, the longitudinal relaxation rate $1/T_1$ is approximately proportional to τ_r and thus to η. In the LiTFSI−EODM-solvent mixture, the TFSI anion can be expected not to interact with any other part of the system in a way seriously affecting its mobility. Accordingly, the relaxation of the four lines of its CF_3 groups in the ^{13}C NMR spectrum should depend only on the viscosity of the system. It can thus be used for normalization of the relaxation times of all other signals to the chosen standard viscosity. We used the normalizing relation between the experimental relaxation time T_{1ex} and the normalized one T_1

$$T_1 = T_{1ex}T_{10}/T_{1C} \tag{19}$$

where T_{10} and T_{1C} are the relaxation times of the central CF_3 signals in 1 M solution of LiTFSI in the given pure solvent and in the actual system, respectively.

The molar fractions of the pure solvent obtained using eqs 13 and 19 and the curves obtained by fitting K_s, K_1, K_2, and n using eq 15 are given in Figure 15. In the case of PC, the relaxation of both carbonyl as well as methyl carbons were used, whereas methyl carbons were available only for DMSO. Since the best value of n obtained both for PC and DMSO was near 4, n was fixed to this value and the remaining three parameters were refitted. The optimized values of K_s, K_1, and K_2 are given in Table 3 together with the values of K_3 obtained using eq 17. As one can see, the method is not very sensitive to the differences between the two models so that even ^{13}C relaxation could not give the ultimate answer to the question why the ester groups of EODM participate in the lithium coordination at higher relative concentrations of PC. Furthermore, in view of the approximation contained in eq 19, the values of K_i obtained in this way must be considered to be indicative only. Notwithstanding this, the semiquantitative conclusion can be made that the effectiveness of DMSO as a ligand is comparable to that of

TABLE 3: The Values of Equilibrium Constants[a] Obtained from Relaxation Measurements and Mathematical Models Excluding (a) or Including (b) Mixed Coordination

	PC		DMSO	
	a	*b*	*a*	*b*
K_s	2.6[0.5]	2.8[0.5]	33.7[0.8]	34.2[0.9]
K_1	26.4[0.9]	28.3[0.9]	24.9[1.1]	27.1[1.3]
K_2	16.8[1.1]	14.9[1.2]	14.7[1.3]	13.3[1.3]
K_3		3.8[0.6]		7.8[0.6]

[a] Fitting errors given in square brackets.

EODM and substantially larger than that of PC. This is quite in agreement with the qualitative conclusions obtained from the patterns of NMR spectra. It has to be noted that a similar superiority of DMF over PC has been observed in plasticized polymer electrolytes.[29]

Conclusions

According to our results, EODM offers several different coordination sites for the lithium ion which are in a swift if not quite free exchange with the solvent. Their relative importance depends on the nature and relative concentration of the solvent, DMSO being a substantially better ligand than PC. The mobility of the lithium ion resident on EODM is markedly reduced in comparison to its mean value in the system. At lower concentrations of PC (less than 35%), relatively immobilized lithium ions occur with residence times 10^{-6} s or higher, which are eventually exchanged with more mobile sites. No permanently immobilized ions could be detected by our methods. This indicates that the favorable influence of the solvent on the performance of a gel electrolyte is not only in its plasticizing effect but also in its ability to losen the coordination of the lithium ion by the poly(ethylene oxide) moiety. DMSO is again more effective than PC in this respect.

Acknowledgment. The authors thank the Academy of Sciences of the Czech Republic for its financial support given under Grant K2050602/12, the Swedish Royal Academy of Science, and the Swedish Natural Science Research Council (NFR).

References and Notes

(1) Wright, P. V. *Br. Polym. J.* **1975**, *7*, 319.
(2) Armand, M. B. *Annu. Rev. Mater. Sci.* **1986**, *16*, 245.
(3) Mac Callum, J. R., Vincent. C. A., Eds. *Polymer Electrolyte Reviews 1*; Elsevier Applied Science: London, 1987.
(4) Callum, J. R., Vincent, C. A., Eds. *Polymer Electrolyte Reviews 2*; Elsevier Applied Science: London, 1989.
(5) Grey, F. M. *Solid Polymer Electrolytes: Fundamentals and Technological Applications*; VCH Publishers: New York, 1991.
(6) Bruce, P. G., Ed. *Solid State Electrochemistry*; Cambridge University Press: Cambridge, 1995.
(7) Reiche, A.; Tübke, J.; Siury, K.; Sandner, B.; Fleischer, G.; Wartewig, S.; Shashkov, S. *Solid State Ionics* **1996**, *85*, 121.
(8) Blint, R. J. *J. Electrochem. Soc.* **1997**, *144*, 787.
(9) Wang, Z.; Huang, B.; Wang, S.; Xue, R.; Huang, X.; Chen, L. *J. Electrochem. Soc.* **1997**, *144*, 778.
(10) Forsyth, M.; Meakin, P.; MacFarlane, D. R. *J. Mater. Chem.* **1997**, *7*, 193.
(11) Huang, W.; Frech, R.; Johansson, P.; Lindgren, J. *Electrochim. Acta* **1995**, *40*, 2147.
(12) Gejji, S. P.; Johansson, P.; Tegenfeldt, J.; Lindgren, J. *Comput. Polym. Sci.* **1995**, *5*, 99.
(13) Ferry, A.; Oradd, G.; Jacobsson, P. *J. Chem. Phys.* **1998**, *108*, 7426.
(14) Williamson, M. J.; Southall, J. P.; Ward, I. M. *J. Chem. Phys.* **1998**, *109*, 7893.
(15) Abbrent, S.; Lindgren, J.; Tegenfeldt, J.; Wendsjö, Å. *Electrochim. Acta* **1998**, *43*, 1185.
(16) Bernson, A.; Lindgren, J. *Solid State Ionics* **1996**, *86*−*88*, 369−372.
(17) Abbrent, S.; Lindgren, J.; Tegenfeldt, J.; Forneaux, J.; Wendsjö, Å. *J. Electrochemical Soc.* **1999**. In press.
(18) Johansson, P.; Gejji, S. P.; Tegenfeldt, J.; Lindgren, J. *Solid State Ionics* **1996**, *86*−*88*, 297.
(19) Johansson, P.; Tegenfeldt, J.; Lindgren, J. *J. Phys. Chem.* **1998**, *102*, 4660−4665.
(20) Johansson, P.; Tegenfeldt, J.; Lindgren, J. *Polymer*. **1999**. In press.
(21) Schmidt, M. W.; Baldridge, K. K.; Boatz, J. A.; Elbert, S. T.; Gordon, M. S.; Jensen, J. J.; Koseki, S.; Matsunaga, N.; Nguyen, K. A.; Su, S.; Windus, T. L.; Dupuis, M.; Montgomery, J. A. *J. Comput. Chem.* **1993**, *14*, 1347.
(22) Bull, T. E. *J. Magn. Reson.* **1972**, *8*, 344.
(23) Deverel, C.; Morgan, R. E.; Strange, J. H. *Mol. Phys.* **1970**, *18*, 553.
(24) Kříž, J.; Dybal, J.; Vlèek, P.; Janata, M. *Macromol. Chem. Phys.* **1994**, *195*, 3039.
(25) Jung, K. J.; Tauskela, J. S.; Katz, J. *J. Magn. Reson. B* **1996**, *112*, 103.
(26) Bowden, G. J.; Hutchison, W. D. *J. Magn. Reson.* **1986**, *67*, 403.
(27) Eliav, U.; Navon, G. *J. Magn. Reson.* **1996**, *A123*, 32.
(28) Jung, K. J.; Katz, J. *J. Magn. Reson. B* **1996**, *112*, 214.
(29) Forsyth M.; et al. *Solid State Ionics* **1996**, *85*, 209; *Solid State Ionics* **1996**, *86*−*88*, 1365.